JOURNAL OF MAGNETIC RESONANCE **134,** 180–183 (1998)
ARTICLE NO. MN981489

Investigation of the Anisotropy in Frozen Nickel Ferrite Ionic Magnetic Fluid Using Magnetic Resonance

J. F. Saenger,* K. Skeff Neto,* P. C. Morais,* M. H. Sousa,† and F. A. Tourinho†

*Instituto de Física, Núcleo de Física Aplicada, Universidade de Brasília; and †Departamento de Química, Universidade de Brasília, 70910-900 Brasília, DF, Brazil

Received December 10, 1997; revised April 6, 1998

Magnetic resonance is used to obtain the temperature dependence of the magnetic anisotropy of noninteracting $NiFe_2O_4$ nanoparticles from 100 to 250 K. The 10.3 nm particles are dispersed as a stable ionic magnetic fluid which is frozen under the action of an external field to perform angular variation measurements. The thermal fluctuation of the easy axis and magnetic moment about the direction of the external field is included in order to obtain the anisotropy from the angular dependence of the resonance field. © 1998 Academic Press

We report on the temperature dependence of the magnetic anisotropy of a $NiFe_2O_4$ nanoparticle obtained from magnetic resonance measurements. The 10.3 nm diameter particle is dispersed as ionic magnetic fluid, diluted enough to prevent particle–particle interaction, thus allowing the investigation of the anisotropy of a single particle in the temperature range from 100 to 250 K. The methodology used to analyze the angular dependence of the magnetic resonance field, in the thermal-locked and thermal-unlocked approximation of the easy axis and magnetic moment, is presented. The values we obtained for the anisotropy of the nanosized particle are smaller than the values reported for bulk samples over the range of temperature of our experiment.

Magnetic fluids are ultrastable material systems composed of monodomain nanosized magnetic particles dispersed as single entities in a liquid carrier. Magnetic fluid stability works against magnetic dipole interaction that tends to stick particles together. Different repulsion mechanisms are used to prevent particle–particle agglomeration, thus leading to different types of magnetic fluids. Steric repulsion prevents agglomeration in surfacted magnetic fluids while coulombic repulsion accounts for stability in ionic magnetic fluids (*1*). Magnetic anisotropy, saturation magnetization, and particle size profile are the basic properties used to characterize a magnetic fluid sample. As far as technological applications of magnetic fluids are concerned, magnetic anisotropy plays a central role. Magnetic anisotropy determines, for instance, magnetization reversal of the nanosized particles and thus the stability of stored information in high-density magnetic storage media. Typical experiments used to measure magnetic anisotropy in nanoscaled magnetic particles include the temperature decay of remanence (*2*), Mössbauer spectroscopy (*3*), and magnetization curves (*4*). In this work the temperature dependence of the saturation magnetization and angular variation of the magnetic resonance spectra of noninteracting $NiFe_2O_4$ nanoparticles, using a diluted nickel ferrite-based ionic magnetic fluid, is obtained. Angular variation of the magnetic resonance spectra, taken from a field-cooled sample, was used to obtain the magnetic anisotropy as a function of temperature. Rigid dipole approximation as well as nonrigid dipole approximation is used to fit the angular variation data, thus leading to the determination of the magnetic texture coefficient, for field-cooled magnetic fluid samples.

Magnetic resonance was recently introduced as a useful technique to measure anisotropy of magnetic nanoparticles (*5*). To perform such a measurement in a straightforward way one needs to prepare the sample so it is as close as possible to an ideal system composed of noninteracting magnetic particles dispersed in a solid nonmagnetic matrix. The easy axis (e.a.) of magnetization associated to the particles must be oriented, as perfectly as possible, parallel to a given direction, in order to fit the requirements of the theoretical models discussed below. Such conditions can be reached with a magnetic fluid sample having particle concentration up to 3×10^{16} particle/cm^3, field-cooled in an external field set above 1 T (*6*). In our experimental setup the sample holder is allowed to rotate around the vertical axis, θ being the angle between the easy axis of the sample and the horizontal external magnetic field (H_e). The resonance frequency ω_r, i.e., the Larmor precession frequency of the magnetic moment (μ) of the particle in the presence of an effective magnetic field (H_{eff}), is given by

$$\omega_r = \gamma H_{eff}, \qquad [1]$$

where γ is the gyromagnetic ratio. In our experiment we scanned the magnetic field strength instead of scanning the microwave frequency. The effective field is a result of three components; the external sweeping field (H_e), the anisotropy field (H_a), and the fluctuation field (H_f). In the general case, including temperature range above and below the characteristic nanoparticle blocking temperature, the anisotropy field and the

1090-7807/98 $25.00

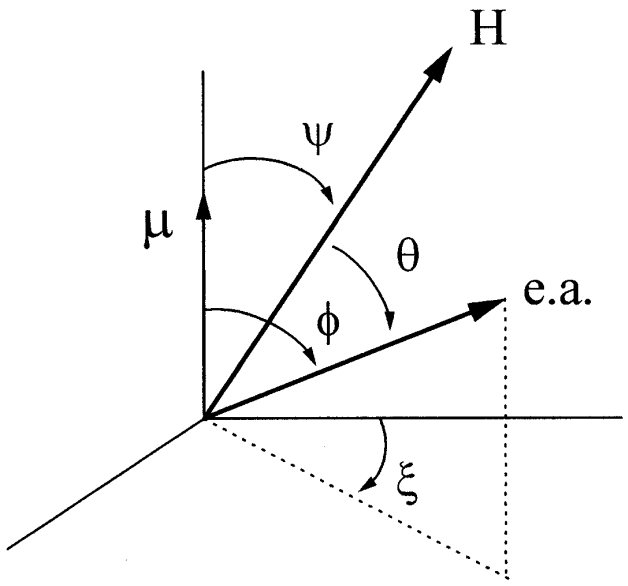

FIG. 1. Schematic representation of the relative orientation of the external applied field, easy axis, and magnetic moment.

fluctuation field are both expected to play a very important role. The temperature dependence of the anisotropy field and the temperature dependence of the fluctuation field can be theoretically evaluated using a statistical ensemble where the thermal fluctuation of the anisotropy axis and magnetic moment is described through an appropriate orientational distribution function. The fluctuation field of a very particular ensemble of monodisperse, noninteracting, rigid dipole nanoparticles in a fluid matrix can be analytically calculated using the Landau–Lifschitz equation to describe the dynamics of the magnetic moment (*7*). The approximative calculation presented here, however, starts with a magnetic fluid sample composed of rigid dipole nanoparticles, cooled down under the action of a high magnetic field. In this condition the fluctuation field has a negligible contribution to the effective field and the resonance condition includes the external field and the anisotropy field only. The anisotropy field reduces to $H_a = (2V/\mu)K$, where the magnetic moment per particle (μ) is related to the saturation magnetization (I_S) by $\mu = I_S V$ and V is the particle volume. Within this approximation the magnetic anisotropy can be expanded in terms of spherical harmonics (*8*),

$$K = \sum_l \sum_m K_l P_l^m(\cos\,\theta) e^{im\varphi}, \qquad [2]$$

where $P_l^m(\cos\,\theta)$ are Legendre polynomials and K_l are anisotropy coefficients. For uniaxial particles one retains only the $l = 2$ term. In the case of spherical particles one retains only the $m = 0$ term. Under the above-mentioned conditions, the anisotropy can be written as $K = K_2 P_2^0(\cos\,\theta)$ and the anisotropy field approximated by $H_a = (2V/\mu)K_2 P_2^0(\cos\,\theta)$. Substituting the anisotropy field expression as described by Eq. [2] into Eq. [1], we obtain the description of the angular dependence of the resonance field,

$$H_r = \left(\frac{\omega_r}{\gamma}\right) - \frac{K}{I_S}(3\,\cos^2\theta - 1). \qquad [3]$$

To complete our approximative calculation, the rigid dipole as well as the high magnetic field condition are both relaxed. The easy axis and the magnetic moment are no longer locked. This leads to an angular distribution of the easy axis of the particle with respect to the external field as well as to an angular distribution of the magnetic moment of the particle with respect to the easy axis, as shown schematically in Fig. 1. To account for the angular distribution we average out the orientation of the easy axis with respect to the applied field using classical statistics. A magnetic texture coefficient defined by $J(T) = \langle\cos^2\theta\rangle$ is then used to include thermal effects and thus to correct the magnetic anisotropy. The description of the temperature dependence of $J(T)$ starts by writing down the free energy (E) of the particle as $E = KV\sin^2\phi - \mu H\cos\psi$. Taking $a = KV/kT$ and $b = \mu H/kT$, the texture coefficient reads

$$J(T) = (2\pi Z)^{-1}\int_0^{2\pi}\int_0^{\pi}\int_0^{\pi}\sin\psi\,\sin\phi\,\cos^2\theta \times \exp(-a\,\sin^2\phi + b\,\cos\,\psi)d\phi d\psi d\xi, \qquad [4]$$

where

$$Z = \int_0^{\pi}\int_0^{\pi}\sin\psi\,\sin\phi\,\exp(-a\,\sin^2\phi + b\,\cos\,\psi)d\phi d\psi$$

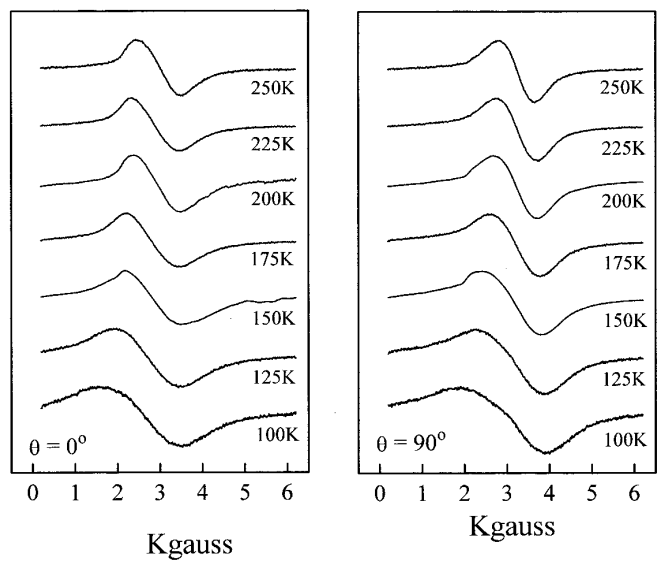

FIG. 2. Typical resonance spectra at different temperatures and different orientation of the sample axis with respect to the external applied field.

is the partition function and $\cos\theta = \cos\psi\cos\phi + \sin\psi\sin\phi\cos\xi$ (see Fig. 1). After the algebraic manipulations are performed, the texture coefficient can be written as

$$J(T) = \frac{L(b)}{b} - \left[\frac{3L(b)}{b} - 1\right]\left[\frac{\exp(a)}{aI(a)} - \frac{1}{2a}\right], \qquad [5]$$

where $L(b) = \coth(b) - (1/b)$ is the Langevin function and $I(a) = \int_{-1}^{+1}\exp(ax^2)dx$. Note that $J(T)$ tends to unity as $a \gg 1$ and $b \gg 1$, corresponding to a system composed of rigid dipole nanoparticles, cooled down under the action of a high magnetic field. Under this very particular condition the angular variation of the magnetic resonance field is perfectly described through Eq. [3]. However, if considerable thermal fluctuation occurs, Eq. [3] is no longer valid and has to be corrected to include the texture coefficient in the following form:

$$H_r = \left(\frac{\omega_r}{\gamma}\right) - J(T)\frac{K}{I_S}(3\cos^2\theta - 1). \qquad [6]$$

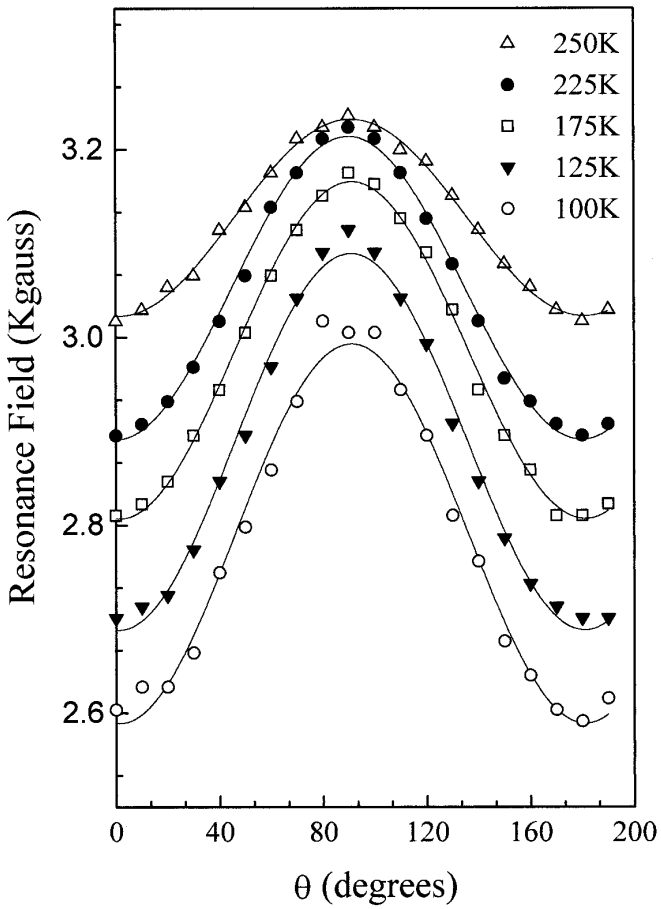

FIG. 3. Angular dependence of the resonance field at different temperatures. The solid lines represent the best fit of the experimental data according to Eq. [6].

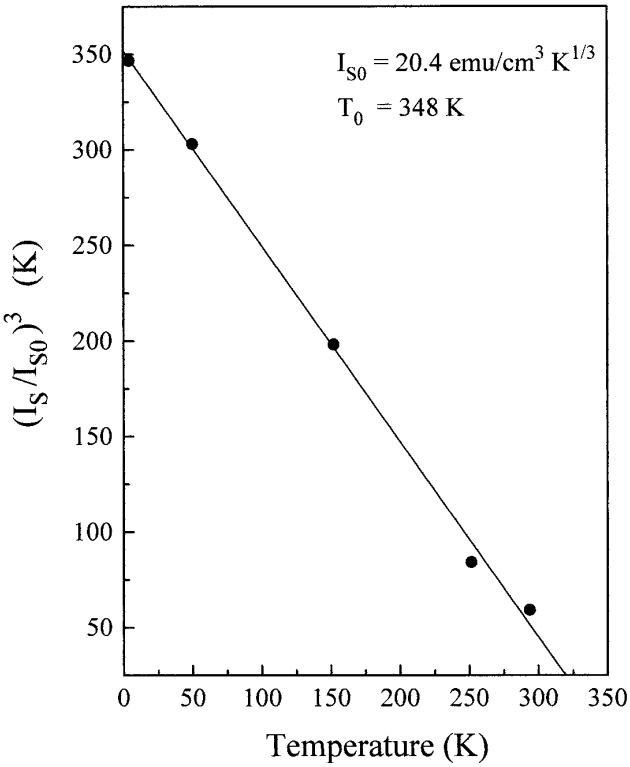

FIG. 4. Reduced saturation magnetization vs temperature.

Equation [6] describes the angular variation measurements in a broad range of temperature and will be used to fit our experimental data in order to obtain the temperature dependence of the effective anisotropy (K).

The chemical synthesis of high-quality $NiFe_2O_4$ based ionic magnetic fluid has been obtained only recently (*9*). The sample used in our experiment was prepared using the condensation method by coprecipitating aqueous solutions of nickel and iron salts in an alkaline medium, followed by peptization of the spherical nanoparticles in water. The particle polydispersity follows a log-normal distribution characterized by a mean particle diameter and a dispersion factor on the order of 10.3 nm and 0.2, respectively. The polydispersity parameters were estimated from X-ray measurements as discussed elsewhere (*9*). The blocking temperature, estimated from Mössbauer measurements, is on the order of 97 K (*10*). For the purpose of magnetic resonance measurements the particle concentration in the magnetic fluid sample was set at 1×10^{16} particles/cm^3. The sample was initially cooled down to 100 K under the action of an external horizontal field of 1.5 T. The sample holder was attached to a goniometer mounted vertically to allow full rotation around the axis perpendicular to the horizontal plane. Magnetic resonance spectra were taken using a X-band spectrometer tuned at 9.428 GHz. At a fixed temperature, magnetic resonance spectra were taken in steps of 10° through rotation of the goniometer axis. Typical resonance spectra are shown in Fig. 2. The resonance fields were obtained

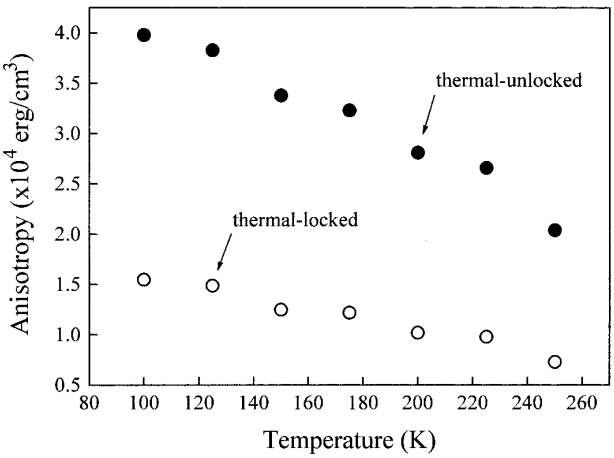

FIG. 5. Temperature dependence of the absolute value of the magnetic anisotropy. Solid circles represent the values obtained using Eq. [6] while open circles represent the values obtained using Eq. [3].

by fitting the spectra using the first derivative of a Gaussian-shaped curve. Values of the resonance field, at different temperatures, as a function of the angle between the original orientation (easy axis of the sample) and the external field are plotted in Fig. 3. Magnetization curves were obtained using a VSM system operating up to 9 T. The saturation magnetization was then obtained at different temperatures by fitting the magnetization vs field curve through a Langevin function. The temperature dependence of the saturation magnetization follows nicely the one-third power law in the range of our data, as shown in Fig. 4. The saturation magnetization curve was adjusted using $I_S = I_{S0}(T_0 - T)^{\beta}$, with $I_{S0} = 20.4$ emu/cm$^3 \times$ K$^{1/3}$, $T_0 = 348$ K, and $\beta = 0.33$. From the angular dependence of the resonance field data and from the saturation magnetization data, at a given temperature, one can use either Eq. [3] or Eq. [6] to obtain the magnetic anisotropy. The solid lines going through the points of Fig. 3 represent the best fit of the experimental data according to Eq. [6]. Equation [3] has been used to fit the angular dependence of the resonance field as well. The temperature dependence of the absolute value of the magnetic anisotropy as obtained from the two fitting procedures, using Eqs. [3] and [6], is shown in Fig. 5. The values we found from our measurements of the effective magnetic anisotropy are smaller than the values reported in the literature for the bulk sample above 100 K (*11*).

In summary, this is the first time magnetic resonance has been used to obtain the effective magnetic anisotropy of non-interacting $NiFe_2O_4$ nanoparticles dispersed as ionic magnetic fluid. The methodology used to analyze the angular variation data, including the effect of thermal fluctuation of the easy axis and magnetic moment, is presented. Indeed, we found that the texture coefficient decreases from 0.39 ± 0.03 at 100 K down to 0.36 ± 0.02 at 250 K, as expected from Eq. [5].

ACKNOWLEDGMENTS

This work was supported by the Brazilian agencies FAPDF, PADCT, CAPES, and CNPq.

REFERENCES

1. F. A. Tourinho, R. Franck, R. Massart, and R. Perzynski, *Prog. Colloid Polym. Sci.* **79,** 128 (1989).
2. R. V. Upadhyay, K. J. Davis, S. Wells, and S. W. Charles, *J. Magn. Magn. Mater.* **132,** 249 (1994).
3. H. R. Rechenberg and F. A. Tourinho, *Hyper. Int.* **67,** 627 (1991).
4. S. Gangopadhyay, G. C. Hadjipanayis, B. Dale, C. M. Sorensen, K. J. Klabunde, V. Papaefthymiou, and A. Kostikas, *Phys. Rev. B* **45,** 9778 (1992).
5. A. F. Bakuzis, P. C. Morais, and F. A. Tourinho, *J. Magn. Res. A* **122,** 100 (1996).
6. P. C. Morais, M. C. F. L. Lara, A. L. Tronconi, F. A. Tourinho, A. R. Pereira, and F. Pelegrini, *J. Appl. Phys.* **79,** 7931 (1996).
7. Yu. L. Raikher and M. I. Shliomis, *Adv. Chem. Phys.* **87,** 595 (1994).
8. H. B. Callen and E. R. Callen, *J. Phys. Chem. Solids.* **27,** 1271 (1966).
9. F. A. Tourinho, P. C. Morais, M. H. Sousa, and L. G. Macedo, *in* ''Proceedings of the Third International Conference on Intelligent Materials and Third European Conference on Smart Structures and Materials,'' Lyon, 1996 (P. F. Gobin and J. Tatibouet, Eds.), SPIE Vol. 2779, p. 317 (1996).
10. J. H. Dias Filho, H.-D. Pfannes, S. L. Pereira, J. L. López, P. C. Morais, A. L. Tronconi, F. A. Tourinho, A. A. Mendes Filho, and L. C. B. de Miranda Pinto, *Hyper. Int. C* **2,** 172 (1997).
11. D. W. Healy, Jr., *Phys. Rev.* **86,** 1009 (1952).